34th Annual International Conference of the IEEE EMBS
San Diego, California USA, 28 August - 1 September, 2012

Information Theoretic Inference of the Optimal Number of Electrodes for Future Cochlear Implants Using a Spiral Cochlea Model

Alexey S. Moroz[1], Mark D. McDonnell[2], Anthony N. Burkitt[3], David B. Grayden[3], Hamish Meffin[4]

Abstract— **Contemporary cochlear implants stimulate the auditory nerve with an array of up to 22 electrodes. More electrodes do not typically provide improved hearing performance. Given that this limitation is primarily due to current spread, and that newly developing kinds of electrodes may enable more focused stimulation, we recently proposed an information theoretic modeling framework for estimating how many electrodes might achieve optimal hearing performance under a range of assumptions about electrodes and their placement relative to the nerve. Here, we extend this approach by introducing more realistic three-dimensional spiral geometries for the cochlea and array, and comparing the optimal number of electrodes predicted by our model for this case with that in our original model, which used a linear geometry.**

I. INTRODUCTION AND BACKGROUND

Cochlear implants [1], [2] can restore hearing when deafness has been caused by the loss of *inner hair cells* in the cochlea (inner ear). In a healthy ear, these cells transduce sounds into action potentials in fibers of the auditory nerve, which propagate to the brain where they are processed and perceived as sound. The purpose of a cochlear implant is to mimic the behavior of missing hair cells via a microphone linked to an array of electrodes that are surgically implanted in the inner ear. Electrical current produced by the electrodes spreads through the inner ear and evokes action potentials in the auditory nerve that are interpreted by the brain as sounds.

An unresolved problem in the design of cochlear implants is that of how many electrodes are needed to achieve the best hearing performance in patients. The limiting factor is that more electrodes mean increased overlapping of stimulation of populations of fibers within the auditory nerve [1]. This problem is often referred to as 'current spread' [3]. Future technologies may allow reduced current spread and more electrodes used to transmit more detailed sound information to the auditory nerve.

We have recently developed an information theoretic approach to determining the optimal number of electrodes, and their positions along the basilar membrane for a simple one-dimensional cochlea model and linearly attenuated current spread [4]. This approach relies on the assumption that spike generation is stochastic. We note that while stochastic spontaneous action potential generation is prevalent in auditory nerve fibers in normal hearing [5], it is significantly diminished in people with profound sensorineural hearing loss [6], [7]. Nevertheless, the generation of action potentials in response to cochlear implant electrode current is well-modelled as a stochastic process [3], [8].

A. Overview of modeling framework

Our approach, as introduced in [4], is to model the electrode to nerve fiber interface as an information theoretic *discrete memoryless channel* (DMC) [9]. While specific elements of this approach are based on an existing stochastic model of electrically evoked auditory nerve activity [10], the overall modeling framework is very general and does not rely on this specific choice. Improvements to any of the framework's individual components can be introduced straightforwardly into future extensions, while maintaining the core concepts.

At this stage, we assess only electrode discriminability. The metric we use is *mutual information* [9]—the motivation and caveats of using this metric are discussed in detail elsewhere, e.g. [11], [4], [12]. Different assumptions for the number of electrodes and electrode array placement can be compared using this quantity [4].

The framework has five separable component models:

1) fiber and electrode array geometry and topology;
2) stochastic electrically evoked action potentials in individual nerve fibers from a current pulse;
3) current spread in the cochlea;
4) loudness perception;
5) electrode place discrimination perception.

In this paper, Components 2-5 are the same as used in [4], and further details can be found therein. However, we make a significant improvement to Component 1.

B. Original model of geometry and topology

In this paper, we study the case where the model's Component 1 comprises a three-dimensional geometry, namely a three-dimensional Archimedian spiral, or helix. This extends the model of [10], [4], in which topology and the location of

The work of Mark D. McDonnell was supported by an Australian Research Fellowship funded by the Australian Research Council (project number DP1093425). The Bionics Institute acknowledges the support it receives from the Victorian Government through its Operational Infrastructure Support Program.

[1]A. S. Moroz is with Moscow Institute of Physics and Technology (State University) and Institute for Telecommunications Research, University of South Australia, Mawson Lakes SA 5095, Australia.

[2]M. D. McDonnell is with the Institute for Telecommunications Research, University of South Australia, Mawson Lakes SA 5095, Australia. mark.mcdonnell@unisa.edu.au

[3]A.N. Burkitt and D.B. Grayden are with the NeuroEngineering Laboratory in the Department of Electrical and Electronic Engineering and the Centre for Neural Engineering at the University of Melbourne, VIC 3010, Australia, and hold honorary appointments at the Bionics Institute, East Melbourne, VIC 3002, Australia.

[4]H. Meffin is with NICTA (National Information & Communication Technology Australia), Melbourne VIC 3010, Australia, and holds an honorary position in the Department of Electrical and Electronic Engineering at the University of Melbourne.

electrodes and fibers were a highly simplified linear model, as is now described.

The notation that was introduced for the linear two-dimensional model in [4] can still be used for an arbitrary geometry as follows. Let the total number of auditory nerve fibers be N and the total number of electrodes be M. The electrodes are assumed to be point sources on the array. Let the electrode array have total length l and the cochlea have total length L. The along-array location of each electrode and the along-cochlea location of each fiber are both normalized with respect to the total length of the *electrode array*, l. The i–th fiber's normalized location *along the cochlea* is denoted by $x_{\mathrm{f},i} \in \left[0, \frac{L}{l}\right]$. The j–th electrode's normalized location *along the array* is denote by $x_{\mathrm{e},j} \in [0,1]$; note that the start location of the array is the same as that of the cochlea, but there are not necessarily either electrodes or fibers at this zero position. We denote the distance (also normalized with respect to l) between fiber i and electrode j as $d_{i,j}$.

In the simple linear model of [10], the complex three-dimensional spiral shape of the cochlea is treated as though it were 'unwrapped' to a single dimension, so that $l = L =$ 30 mm. In [4], this was extended to a second dimension so that the array and inner wall of the cochlea, the modiolus, are parallel and separated by a distance $r \in [0,2]$ mm. Thus, the total normalized distance between fiber i and electrode j was expressible as a function of r as

$$d_{i,j} = \sqrt{(x_{\mathrm{e},j} - x_{\mathrm{f},i})^2 + \left(\frac{r}{l}\right)^2},\ i = 1,..,N;\ j = 1,..,M. \tag{1}$$

The model of [10] is recovered when $r = 0$. Since this model ignores the complex spiral-shaped geometry of the cochlea, Eqn. (1) will be accurate only for small $|x_{\mathrm{e},j} - x_{\mathrm{f},i}|$ [13], [14]. In this paper, we go beyond this simplified case by considering three-dimensional Archimedial spirals for both the cochlea and electrode array, and therefore we have a more complicated equation for $d_{i,j}$, as described in Section II.

We assume here that there are N fibers uniformly distributed along the cochlea, although the model is easily generalizable to arbitrary fiber densities. Although it is certainly feasible to consider non-uniformly spaced electrodes, we only consider the case where they are uniformly distributed.

II. IMPROVED MODEL: A 3D COCHLEA SPIRAL

The human cochlea forms a three-dimensional spiral with an average unwrapped length of 30 mm, an average height of 2.75 mm, and total twirling angle (i.e., the maximum polar angle) of approximately 5π radians [15], [16]. Here, we model both the cochlea and the electrode array as forming three-dimensional Archimedian spirals. The cochlea spiral has a total twirling angle of $\psi = 5\pi$ radians, while the electrode array has a total twirling angle (denoted as α) that is less than that of the cochlea. We consider two cases: $\alpha = 3\pi$ radians (with a total array length at $r = 0$ mm of $l = 26.6$ mm) and $\alpha = 2\pi$ radians (with a total array length at $r = 0$ mm of $l = 20.2$ mm). The length of the full 5π cochlea spiral will be approximately $L = 33$ mm. The shorter angles of the electrode array were chosen to reflect current surgical techniques and array designs, which are not able to place the electrode array very deep in the cochlea, allowing it to make approximately only one to one-and-a-half turns along the spiral.

An Archimedian spiral for a cochlea with maximum radius $R_{\max}$ from its centre to the auditory nerve fibers, and maximum height $h_{\max}$, has the following formulae for radial distance R and height h for each point on the curve (note that the spiral is twirled counter-clockwise, and all distances are in millimeters):

$$R(\varphi) = R_{\max}\left(1 - \frac{\varphi}{\psi}\right), \quad h(\varphi) = h_{\max}\frac{\varphi}{\psi},$$

where φ describes the angle of all points of the spiral between zero and ψ radians. Knowing the angle value, we can determine R, h, and the length of cochlea in our approximation from the start up to current point. The exact formula for the length $L^{\mathrm{cochlea}}(\varphi)$ is the following:

$$L^{\mathrm{cochlea}}(\varphi) = \frac{k^2}{2\mathrm{a}_2}\begin{pmatrix}\mathrm{t}_0\sqrt{1+{\mathrm{t}_0}^2} + \operatorname{arcsinh}(\mathrm{t}_0) - \\ t\sqrt{1+t^2} - \operatorname{arcsinh}(t)\end{pmatrix},$$
$$\mathrm{k} = \sqrt{{\mathrm{a}_2}^2 + {\mathrm{a}_3}^2}, \mathrm{t}_0 = \frac{\mathrm{R}_{\max}}{k}, t = \frac{\mathrm{R}_{\max} - \mathrm{a}_2\varphi}{k},$$

where $\mathrm{a}_2 = R_{\max}/\psi$ and $\mathrm{a}_3 = h_{\max}/\psi$. We use $R_{\max} =$ 4.0 mm and $h_{\max} = 2.75$ mm.

Similar formulae apply for the electrode array, since it is considered as forming the same spiral, but with greater radial distance, namely $R + r$. The height is the same.

Note that the length of the spiral depends on the angle, φ, in a nonlinear manner. However, it is still possible to use an arbitrary distribution of fibers and even electrodes denoted by normalized distance along the cochlea and array, respectively (recall that we normalized with respect to the *length of the array*), although it would be easier to denote locations by their angles. The values of radius, angle, and height for the i–th fiber along the cochlea and the j–th electrode in the array can be denoted as $\{R_{\mathrm{f},i}, \varphi_{\mathrm{f},i}, h_{\mathrm{f},i}\}$ and $\{R_{\mathrm{e},j}, \varphi_{\mathrm{e},j}, h_{\mathrm{e},j}\}$ accordingly.

The normalized distance between fiber i and electrode j can be written as

$$d_{i,j} = \frac{\begin{bmatrix}((R_{\mathrm{e},j}+r)\cos(\varphi_{\mathrm{e},j}) - R_{\mathrm{f},i}\cos(\varphi_{\mathrm{f},i}))^2 + \\ ((R_{\mathrm{e},j}+r)\sin(\varphi_{\mathrm{e},j}) - R_{\mathrm{f},i}\sin(\varphi_{\mathrm{f},i}))^2 + \\ (h_{\mathrm{e},j} - h_{\mathrm{f},i})^2\end{bmatrix}^{\frac{1}{2}}}{l},$$

where $i = 1,..,N;\ j = 1,..,M$.

III. RESULTS

In this section, we present and discuss results obtained from numerical evaluation of the mutual information, as various parameters, including the number of electrodes, M, are varied in the model. Almost all parameters are the same as in [4]. The primary differences are that here we consider the spiral model of Section II, as well as the linear model of [4] for comparison, and also vary the attenuation model. As before, the distance r between electrode array and fibers

is assumed to be a variable $r \in [0, 2]$ mm. Although it is implausible in reality that r can be made much less than 2 mm, we study this variable to show that the model correctly captures what could be expected to occur if r were varied. The total number of fibers is assumed to be $N = 10000$.

A. The optimal number of electrodes: Comparing linear and spiral geometry

As a first set of results for the spiral geometry introduced in this paper, we compare two different models for current spread for the two primary methods of electrical stimulation: bipolar and monopolar stimulation. Here we are using an isotropic linear-with-distance attenuation model. Values suggested by [10] for this model are $A = 4.0$ dB per mm for bipolar and 0.5 dB per mm for monopolar stimulation. In [4], only $A = 4.0$ dB per mm is considered. In order to determine the level of influence that an improved geometry model has on the outcome, we now compare the linear model with two cases of the spiral model, for a maximum current, $C_{\max}$, and minimum current, $C_{\min}$, each computed as in [4].

We computed the mutual information as a function of radial distance $r \in [0, 2]$ mm and for all electrode array sizes $M = 2, .., 40$ for (i) the linear model; (ii) for the spiral model with a total twirling angle of the electrode array of $\alpha = 2\pi$ radians; and (iii) for the spiral model with $\alpha = 3\pi$ radians. Obtaining the number of electrodes that maximizes the mutual information is one of our primary goals. This information, and the corresponding maximum mutual information, can be easily extracted from numerical data [4]. Figs 1(a) and 2(a) show the optimal number of electrodes as a function of r for both minimum and maximum currents for the monopolar and bipolar models. Figs 1(b) and 2(b) show the mutual information achieved for that optimizing number of electrodes in the array.

For the spiral model with a twirling angle of $\alpha = 2\pi$ radians, the optimal number for monopolar stimulation is 4 or 5 for the minimum current, and between 10 and 14 for the maximum current. For bipolar stimulation, there is a much greater dependence on the array to modiolus distance, r, with a steady increase from 14 electrodes at $r = 2$ mm to 31 electrodes at $r = 0$ for minimum current. For maximum current, the range is from 22 to 39 electrodes.

The results shown in Fig. 2 in the linear case are different numerically from those in [4] for the bipolar case. This is partially because here we use a different array length (it was 30 mm in [4]), but primarily due to the different geometry.

Somewhat surprisingly, for maximum current we conclude that the geometry of the linear model is not significantly poorer than the spiral models. Notice that for maximum current, the $\alpha = 3\pi$ model provides marginally superior mutual information for both stimulation modes for smaller values of r. This is likely due simply to the longer electrode array length, l. Meanwhile, the linear and $\alpha = 2\pi$ performance are almost identical in terms of mutual information. The small difference in the number of electrodes for these two cases can again be put down to different array lengths.

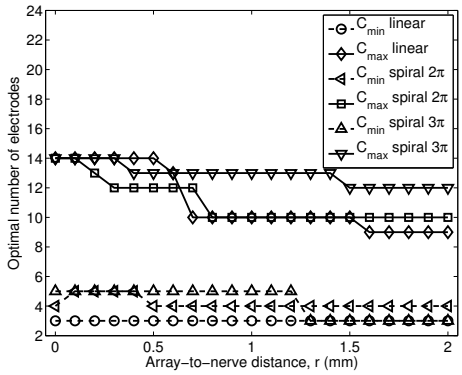

(a) Optimal number of electrodes

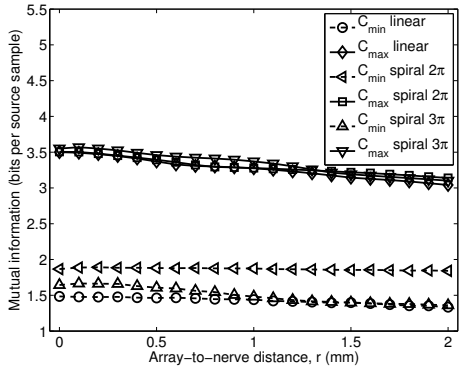

(b) Optimal mutual information

Fig. 1. Comparison of different array topologies for monopolar stimulation ($A = 0.5$). Optimal number of electrodes and the mutual information achieved with the optimal number of electrodes as a function of array-to-nerve distance.

For the minimum current, there are much greater discrepancies between the three models for the mutual information, particularly in the bipolar case. Surprisingly, the $\alpha = 3\pi$ model provides by far the lowest mutual information for minimum current.

We found that monopolar stimulation provides significantly lower mutual information in the model for a broad range of values of r and number of electrodes, M. This result is not unexpected, because the lower attenuation value in the monopolar case means much wider current spread. This results in greater overlap of the number of fibers that are stimulated by each electrode, and thus more ambiguity about the place of stimulation in the model. We discuss this result in Section IV.

IV. DISCUSSION

For the maximum current case, our results did not exhibit great differences between the linear and spiral geometry for the case of bipolar stimulation. The optimal number of electrodes in the model at zero radial distance for the array is approximately 40 for large currents and 30 for small currents. With the linear geometry, optimal numbers were approximately 40 and 20, respectively. Note that in the spiral case, we slightly increased the minimal current in comparison with [4], since it is a free parameter. Nevertheless, the more

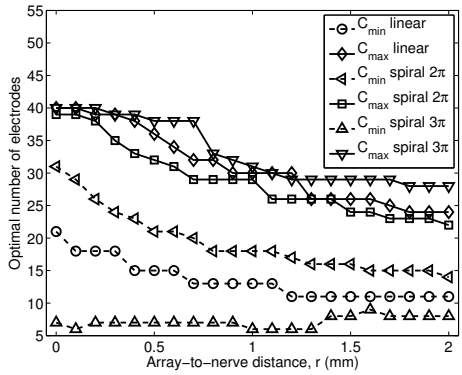

(a) Optimal number of electrodes

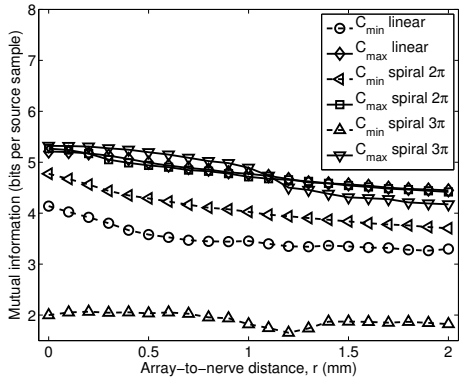

(b) Optimal mutual information

Fig. 2. Comparison of different array topologies for bipolar stimulation ($A = 4.0$). Optimal number of electrodes and the mutual information achieved with the optimal number of electrodes as a function of array-to-nerve distance.

precise geometry of the spiral model narrowed the range for the optimal size of the electrode array.

There remain a number of aspects that are difficult to incorporate into our model. For example, we assume that the conductivity of the cochlea tissue is the same in all directions. As a consequence, electrodes located on the second turn of the spiral have a strong overlap with fibers stimulated by electrodes on the first turn. Modeling of the three-dimensional spiral with a twirling angle of $\alpha = 3\pi$ radians (i.e. with an overlapping angle of π radians) showed that for electrodes located on the "overlapping" region at a radial distance r from the cochlea of about 1.5 mm, the distance to the fibers of the first turn is of the same in the order of magnitude. This results in a significant increase of the mutual information at radial distances r larger than 1.5 mm. This is an issue of isotropic conductivity used in our model. Also, for the twirling angle of $\alpha = 2\pi$ radians, the mutual information can be over-estimated at large distances from the fibers. Since modern surgical techniques and array designs allow placing of the array deeper than only one turn [15], [13], future work could benefit from introduction of an anisotropic conductivity model.

In general, a superior model to that used here would be a three-dimensional mesh covering the entire cochlea with high precision. Of course, the location of all tissues and especially fibers must be based on the results of computed tomography, if possible. Also, attention must be paid to the precise location of the electrode array. The most commonly used arrays resemble a spiral used in our model, but contain rectangular electrodes with a width equal to the width between electrodes and pointed towards the center of the spiral, and are located in the *scala tympani*. It is obvious that conductivity in this case would become anisotropic, so we will need to know the values of conductivity for the *living* tissues of the cochlea and resistances for the transitions between the tissues.

REFERENCES

[1] B. S. Wilson and M. F. Dorman, "Cochlear implants: A remarkable past and a brilliant future," *Hearing Research*, vol. 242, pp. 3–21, 2008.

[2] F. G. Zeng, S. Rebscher, W. Harrison, X. Sun, and H. Feng, "Cochlear implants: System design, integration, and evaluation," *IEEE Reviews in Biomedical Engineering*, vol. 1, pp. 115–142, 2008.

[3] I. C. Bruce, M. W. White, L. S. Irlicht, S. J. O'Leary, and G. M. Clark, "The effects of stochastic neural activity in a model predicting intensity perception with cochlear implants: Low-rate stimulation," *IEEE Transactions on Biomedical Engineering*, vol. 46, pp. 1393–1404, 1999.

[4] M. D. McDonnell, A. N. Burkitt, D. B. Grayden, H. Meffin, and A. J. Grant, "A channel model for inferring the optimal number of electrodes for future cochlear implants," *IEEE Transactions on Information Theory*, vol. 56, pp. 928–940, 2010.

[5] D. H. Johnson and N. Y. S. Kiang, "Analysis of discharges recorded simultaneously from pairs of auditory nerve fibers," *Biophysical Journal*, vol. 16, pp. 719–733, 1976.

[6] M. C. Liberman and L. W. Dodds, "Single-neuron labeling and chronic cochlear pathology. ii. stereocilia damage and alterations of spontaneous discharge rates," *Hearing Research*, vol. 16, pp. 43–53, 1984.

[7] R. P. Morse, P. F. Morse, T. B. Nunn, K. A. M. Archer, and P. Boyle, "The effect of Gaussian noise on the threshold, dynamic range, and loudness of analogue cochlear implant stimuli," *Journal of the Association for Research in Otolaryngology*, vol. 8, pp. 42–53, 2007.

[8] N. S. Imennov and J. T. Rubinstein, "Stochastic population model for electrical stimulation of the auditory nerve," *IEEE Transactions on Biomedical Engineering*, vol. 56, pp. 2493–2501, 2009.

[9] T. M. Cover and J. A. Thomas, *Elements of Information Theory*, 2nd ed. Wiley, New York, 2006.

[10] I. C. Bruce, L. S. Irlicht, M. W. White, S. J. O'Leary, S. Dynes, E. Javel, and G. M. Clark, "A stochastic model of the electrically stimulated auditory nerve: Pulse-train response," *IEEE Transactions on Biomedical Engineering*, vol. 46, pp. 630–637, 1999.

[11] R. Q. Quiroga and S. Panzeri, "Extracting information from neuronal populations: information theory and decoding approaches," *Nature Reviews Neuroscience*, vol. 10, pp. 173–185, 2009.

[12] M. D. McDonnell, S. Ikeda, and J. H. Manton, "An introductory review of information theory in the context of computational neuroscience," *Biological Cybernetics*, vol. 105, pp. 55–70, 2011.

[13] J. J. Briaire and J. H. M. Frijns, "Unraveling the electrically evoked compound action potential," *Hearing Research*, vol. 205, pp. 143–156, 2005.

[14] ——, "The consequences of neural degeneration regarding optimal cochlear implant position in scala tympani: A model approach," *Hearing Research*, vol. 214, pp. 17–27, 2006.

[15] B. M. Verbist, M. W. Skinner, L. T. Cohen, P. A. Leake, C. James, C. Boex, T. A. Holden, C. C. Finley, P. S. Roland, J. T. R. Jr., M. Haller, J. F. Patrick, C. N. Jolly, M. A. Faltys, J. J. Briaire, , and J. H. M. Frijns, "Consensus panel on a cochlear coordinate system applicable in histologic, physiologic, and radiologic studies of the human cochlea," *Otology & Neurotology*, vol. 31, pp. 722–730, 2010.

[16] S. K. Yoo, G. Wang, J. T. Rubinstein, and M. W. Vannier, "Three-dimensional geometric modeling of the cochlea using helico-spiral approximation," *IEEE Transactions on Biomedical Engineering*, vol. 47, pp. 1392–1402, 2000.